



## **Supplementary Information for**

Common sequence motifs of nascent chains engage the ribosome surface and trigger factor.

Annika Deckert<sup>1a</sup>, Anaïs M.E. Cassaignau<sup>1a\*</sup>, Xiaolin Wang<sup>1a</sup>, Tomasz Włodarski<sup>1a</sup>, Sammy H.S. Chan<sup>1</sup>, Christopher A. Waudby<sup>1</sup>, John Kirkpatrick<sup>1</sup>, Michele Vendruscolo<sup>3</sup>, Lisa D. Cabrita<sup>1</sup> and John Christodoulou<sup>1,2,\*</sup>

<sup>1</sup>Institute of Structural and Molecular Biology, University College London, WC1E 6BT London, UK

<sup>2</sup>The Francis Crick Institute, London NW1 1AT, UK

<sup>3</sup>Centre for Misfolding Disease, University of Cambridge, Cambridge CB2 1EW, UK

\*John Christodoulou.

**Email:** [j.christodoulou@ucl.ac.uk](mailto:j.christodoulou@ucl.ac.uk)

### **This PDF file includes:**

Supplementary Text  
Supplementary Figures S1 to S5  
NMR protocols and pulse sequences

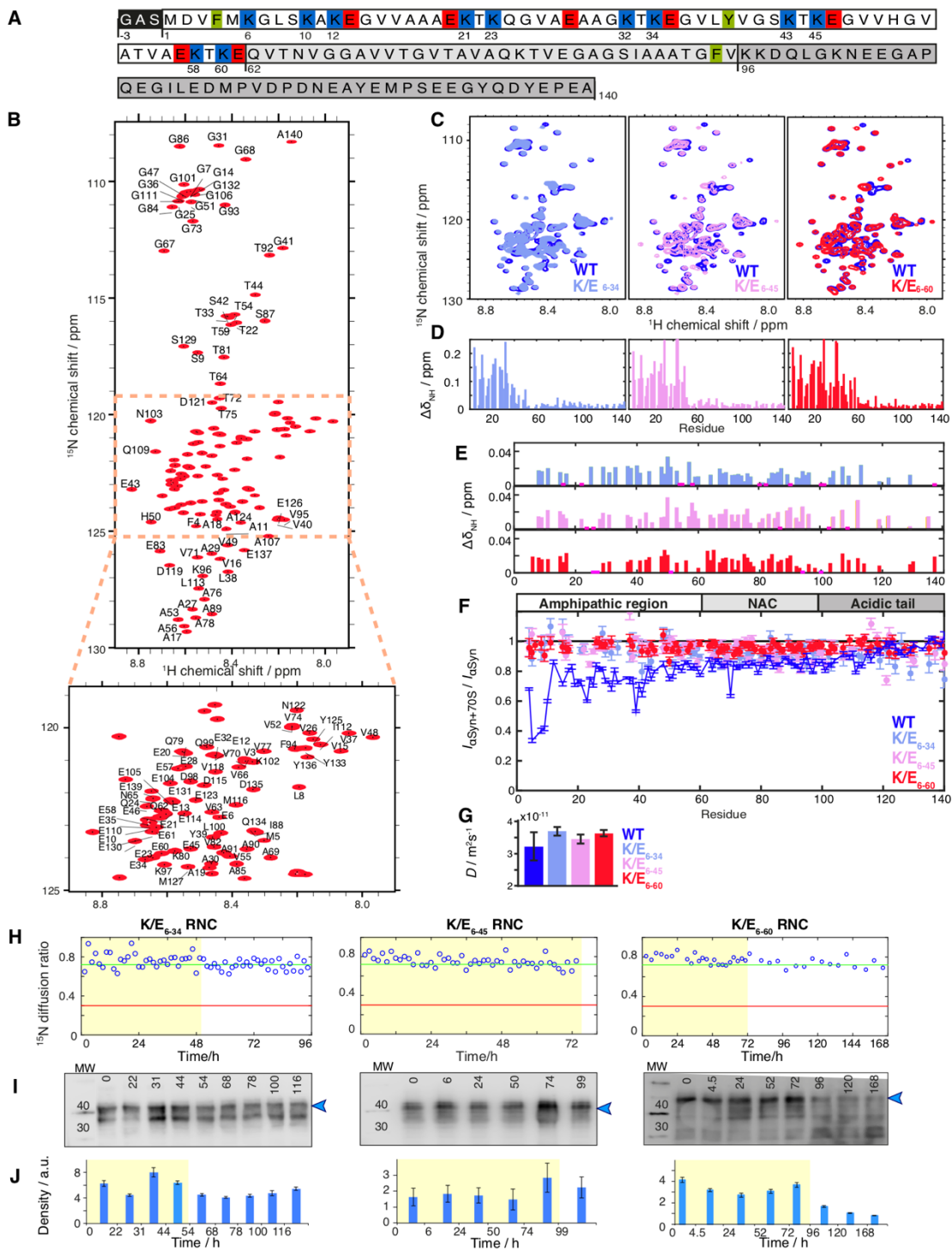


**Figure S1: NMR characterization of the  $\alpha$ Syn K-to-E variant proteins and quality control of the corresponding RNCs during NMR acquisition. (A) WT  $\alpha$ Syn amino acid sequence. Charged residues in the amphipathic region are highlighted in blue (positively-charged) and red (negatively-charged). Aromatic residues that have been mutated to alanines within the K/E<sub>6-60</sub> FYF/AAA constructs have been highlighted in light green. (B) <sup>1</sup>H,<sup>15</sup>N-HSQC spectrum of the K/E<sub>6-60</sub>  $\alpha$ Syn variant including backbone assignment. (C) Overlays of <sup>1</sup>H,<sup>15</sup>N-SOFAST-HMQC spectra of WT**

$\alpha$ Syn (blue) with K/E<sub>6-34</sub> (light blue), K/E<sub>6-45</sub> (pink) and K/E<sub>6-60</sub>  $\alpha$ Syn (red). **(D)**  $\Delta\delta_{\text{NH}}$  chemical shift changes between isolated WT  $\alpha$ Syn and K/E<sub>6-34</sub>  $\alpha$ Syn (light blue), K/E<sub>6-45</sub>  $\alpha$ Syn (pink) and K/E<sub>6-60</sub>  $\alpha$ Syn (red) ( $\Delta\delta_{\text{NH}} = [\Delta\delta_{\text{H}}^2 + (\Delta\delta_{\text{N}}/5)^2]^{1/2}$ ). **(E)**  $\Delta\delta_{\text{NH}}$  chemical shift differences between the isolated K-to-E  $\alpha$ Syn variants in the presence of 70S ribosomes and the K-to-E  $\alpha$ Syn RNC for K/E<sub>6-34</sub> (light blue), K/E<sub>6-45</sub> (pink) and K/E<sub>6-60</sub> (red). Chemical shifts that could be measured but remained unchanged are indicated as magenta boxes. **(F)** Cross-peak intensities of K-to-E mutant  $\alpha$ Syn in the presence of 70S ribosomes relative to K-to-E  $\alpha$ Syn alone for K/E<sub>6-34</sub> (light blue), K/E<sub>6-45</sub> (pink) and K/E<sub>6-60</sub> (red). Relative cross-peak intensities comparing WT  $\alpha$ Syn in the presence and absence of ribosomes have been plotted for comparison (blue). **(G)** Translational diffusion coefficient of the  $\alpha$ Syn protein variants as measured by NMR spectroscopy. **(H)** Intensity ratio  $I_{95\%}/I_{5\%}$  of the mutant  $\alpha$ Syn RNCs during NMR acquisition. The green line represents the intensity ratio measured for intact 70S ribosomes (hydrodynamic radius  $r_h=12.6$  nm (1), diffusion coefficient  $D=1.1 \times 10^{-11}$  m<sup>2</sup>s<sup>-1</sup> at 277 K in H<sub>2</sub>O). The red line indicates the intensity ratio of isolated  $\alpha$ Syn ( $r_h=2.72$  nm (2),  $D=5 \times 10^{-11}$  m<sup>2</sup>s<sup>-1</sup> at 277 K in H<sub>2</sub>O). **(I)** Anti- $\alpha$ Syn western blots of the mutant RNC samples (10 pmol, 70S concentration) collected periodically during NMR acquisition to monitor RNC integrity. The blue arrow indicates the tRNA-attached  $\alpha$ Syn NC. **(J)** The western blots were subsequently analysed by densitometry measurements of the tRNA-bound form (blue arrow) of the NC. The area shaded in yellow indicates the time during which the samples were deemed intact.

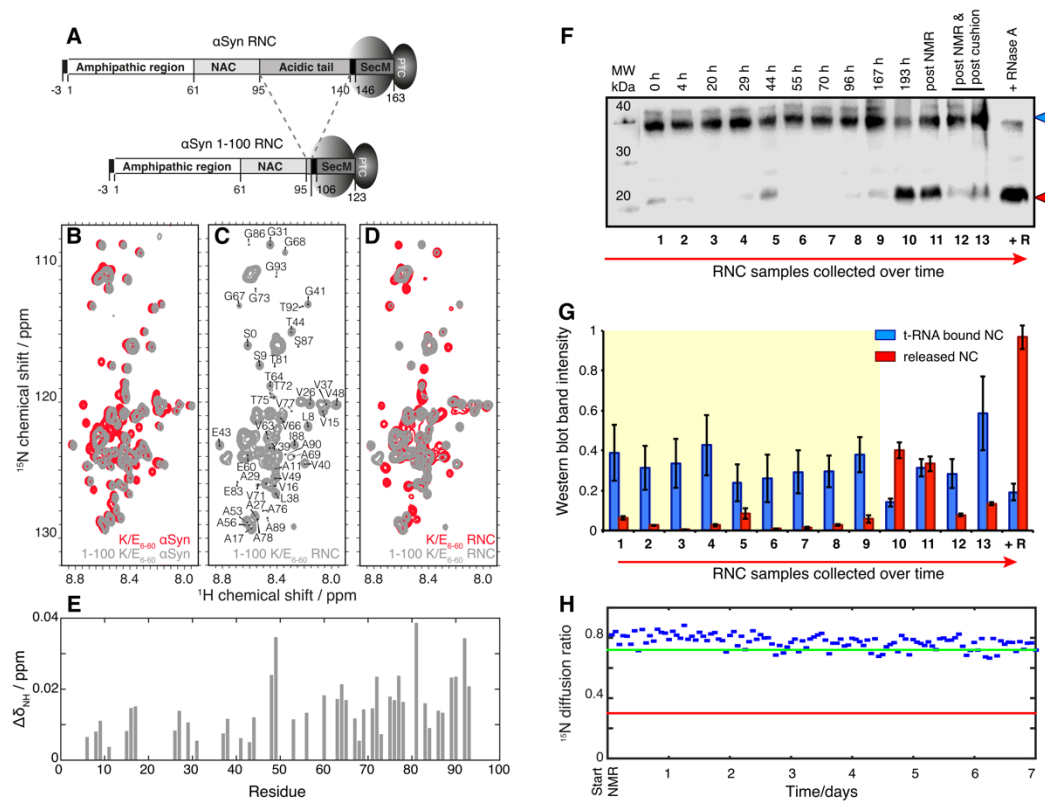


**Figure S2: NMR measurements of the 1-100 K/E<sub>6-60</sub> RNC.** (A) Design of the K/E<sub>6-60</sub> 1-100  $\alpha$ Syn RNC construct, in which the 40 N-terminal residues of the acidic tail have been removed from the  $\alpha$ Syn sequence. (B)  $^1\text{H},^{15}\text{N}$ -SOFAST-HMQC spectra of 5  $\mu\text{M}$  1-100 K/E<sub>6-60</sub>  $\alpha$ Syn (grey) overlaid with 5  $\mu\text{M}$  of the full-length  $\alpha$ Syn protein (red). (C)  $^1\text{H},^{15}\text{N}$ -SOFAST-HMQC spectrum of the 1-100 K/E<sub>6-60</sub>  $\alpha$ Syn RNC (grey) including newly assigned resonances and (D) overlaid with the spectrum of the full-length K/E<sub>6-60</sub>  $\alpha$ Syn RNC (red). (E)  $\Delta\delta_{\text{NH}}$  chemical shift changes between the 1-100 K/E<sub>6-60</sub>  $\alpha$ Syn RNC and the full-length K/E<sub>6-60</sub>  $\alpha$ Syn RNC ( $\Delta\delta_{\text{NH}} = [\Delta\delta_{\text{H}}^2 + (\Delta\delta_{\text{N}}/5)^2]^{1/2}$ ). (F) Anti- $\alpha$ Syn western blot time course of samples collected during NMR acquisition. The blue arrow indicates the tRNA-bound NC, the red arrow the released form. (G) Band intensities of the tRNA-bound and released form of RNC samples loaded in (F) are plotted over time to estimate NC release during NMR acquisition. The area shaded in yellow indicates the time during which the sample was deemed intact. (H) Intensity ratio  $I_{95\%}/I_{5\%}$  of the 1-100 K/E<sub>6-60</sub>  $\alpha$ Syn RNC during NMR data acquisition (average  $I_{95\%}/I_{5\%} = 0.77 \pm 0.04$  and diffusion coefficient  $D = 1.01 \times 10^{-11} \pm 1.2 \times 10^{-12} \text{ m}^2\text{s}^{-1}$ ). As in Figure S1, the green line represents the intensity ratio measured for intact 70S ribosomes and the red line indicates the intensity ratio of isolated  $\alpha$ Syn.

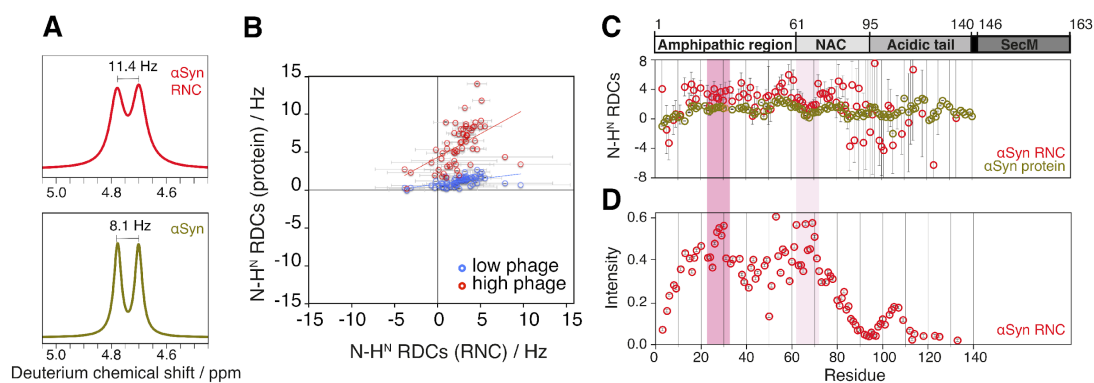


**Figure S3: RDC measurements on the K/E<sub>6-60</sub> RNC.** (A) 1D <sup>2</sup>H spectra of the  $\alpha$ Syn K/E<sub>6-60</sub> RNC in 15.1 mg/mL Pf1 phage (11.4 Hz deuterium splitting) and isolated K/E<sub>6-60</sub>  $\alpha$ Syn in 11.4 mg/mL Pf1 phage (8.1 Hz deuterium splitting). (B) Correlation between RDCs of the K/E<sub>6-60</sub>  $\alpha$ Syn protein and those measured on the K/E<sub>6-60</sub>  $\alpha$ Syn RNC, both in low (11.4 mg/mL for the isolated protein and 15.8 mg/mL for the RNC) and high (24.3 mg/mL for the isolated protein and 24.2 mg/mL for the RNC) concentration phage. (C) N-H<sup>N</sup> RDCs measured on the K/E<sub>6-60</sub>  $\alpha$ Syn RNC (red) and isolated K/E<sub>6-60</sub>  $\alpha$ Syn protein (green). (D) Intensities of the K/E<sub>6-60</sub>  $\alpha$ Syn RNC <sup>1</sup>H,<sup>15</sup>N-HSQC. The shaded pink bars indicate cross-peaks with the highest peak intensity.

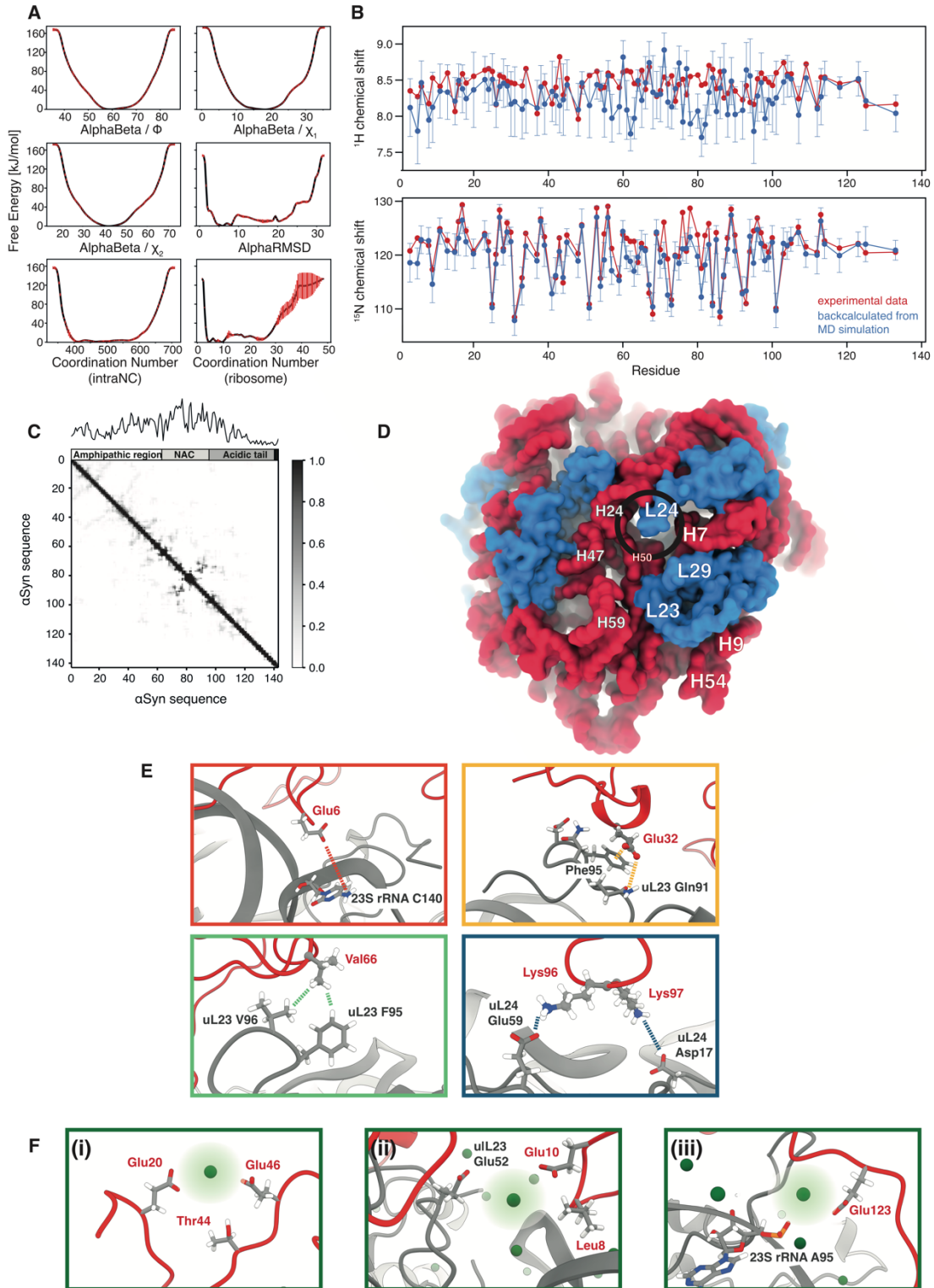


**Figure S4: RDC-restrained all-atom MD simulation of the K/E<sub>6-60</sub> RNC. (A)** Free energy profiles calculated along all 6 CVs, averaged over the last 100 ns of the simulation. Errors: standard

deviations. **(B)** Comparison between the back-calculated  $^1\text{H},^{15}\text{N}$  chemical shifts from MD simulations (blue) and experimentally derived (red). Despite the inevitable limits of MD simulations in terms of the lack of convergence for this complex multi-million-atom system with an intrinsically disordered protein, good agreement between back-calculated backbone amide  $^{15}\text{N}$  chemical shifts is observed with those derived experimentally. **(C)** Contact map characterizing  $\alpha\text{Syn}$  intra-chain interactions. The sum of the contacts is plotted above the contact map. **(D)** The end of the ribosome exit port (circled in black) with a more protein-rich side (RHS, comprises uL23, uL24 and uL29) while the opposite side is predominantly composed of rRNA (LHS). **(E)** Examples of the interactions that the  $\alpha\text{Syn}$  K/E<sub>6-60</sub> NC undergoes with the ribosome surface. The colour of each box matches the rainbow-coding of the circos plot in Fig. 4C. **(F)** Examples of the  $\text{Mg}^{2+}$ -mediated interactions sampled by the  $\alpha\text{Syn}$  K/E<sub>6-60</sub> NC: (i) intra-NC interaction mediated by  $\text{Mg}^{2+}$ , (ii) NC-ribosome interaction mediated by  $\text{Mg}^{2+}$  via a ribosomal protein and (iii) NC-ribosome interaction mediated by the phosphate backbone of a rRNA nucleotide.

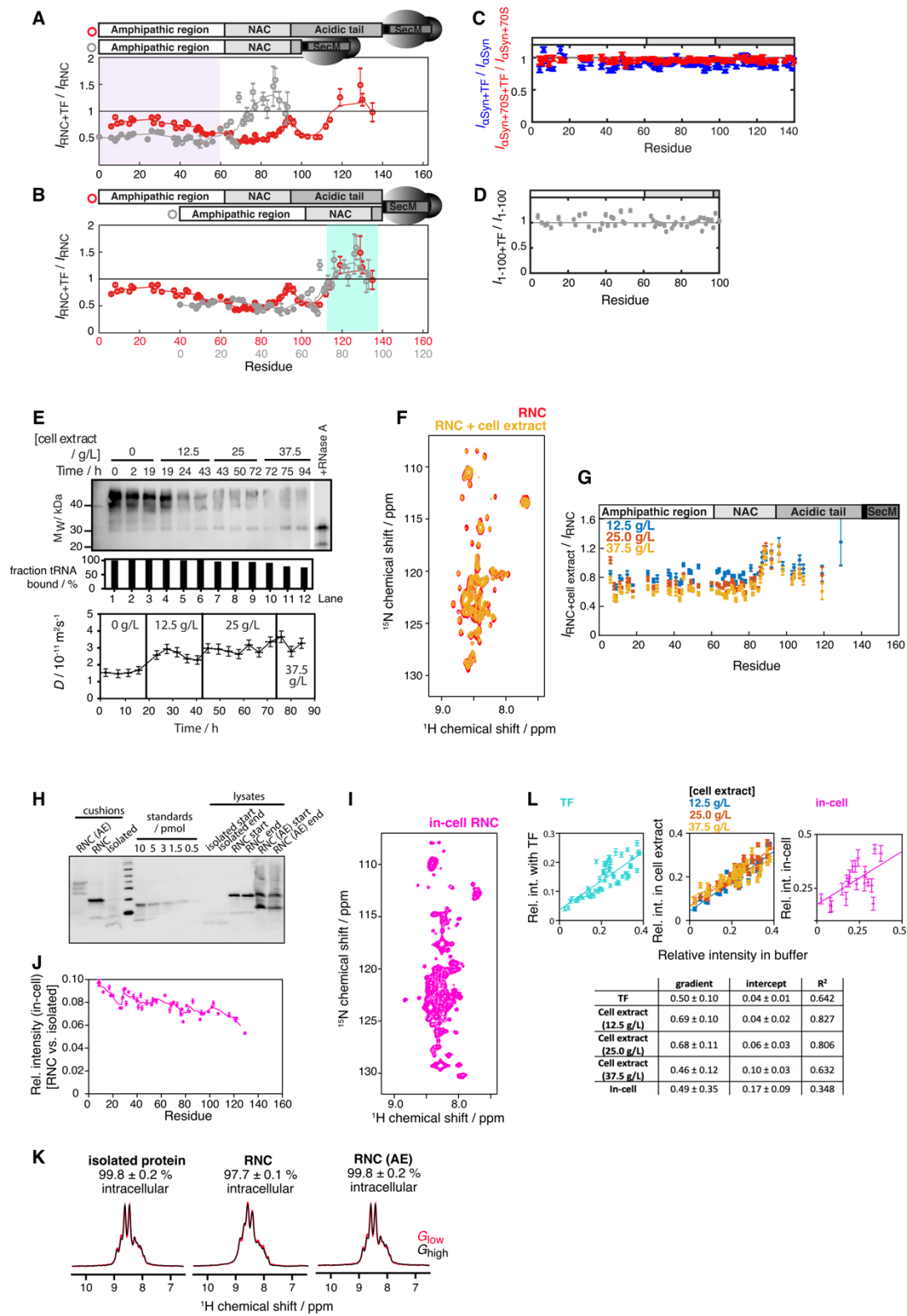




**Figure S5:  $\alpha$ Syn K/E<sub>6-60</sub> RNC in the presence of TF, with cell extract and in-cell. (A)** Relative cross-peak intensities of the 1-100  $\alpha$ Syn K/E<sub>6-60</sub> RNC (grey) and the full-length K/E<sub>6-60</sub>  $\alpha$ Syn RNC (red) in the presence vs in the absence of TF. The N-termini of the NCs have been aligned. 5-point moving averages are plotted. The 60 N-terminal residues, albeit giving rise to a similar intensity pattern, exhibit more severe reductions in intensity for the 1-100 RNC than for the full-length constructs (purple), thought to be due to the reduced distance between the shorter construct and the TF cradle. **(B)** Same as A, except the C-termini of the NCs have been aligned. The cyan shaded area indicates the segment of the  $\alpha$ Syn RNCs that appears unaffected by the presence of the TF chaperone. **(C)** Cross-peak intensities of isolated K/E<sub>6-60</sub>  $\alpha$ Syn in the presence of TF relative to isolated K/E<sub>6-60</sub>  $\alpha$ Syn (blue) and K/E<sub>6-60</sub>  $\alpha$ Syn in the presence of both TF and 70S ribosomes relative to K/E<sub>6-60</sub>  $\alpha$ Syn with ribosomes (red). **(D)** Relative cross-peak intensities of 1-100 K/E<sub>6-60</sub>  $\alpha$ Syn in the presence and absence of 1 molar equivalent of TF. **(E)** Analyses of  $\alpha$ Syn K/E<sub>6-60</sub> RNC sample in cell extract: **(upper)** Anti- $\alpha$ Syn western blot of samples taken during NMR acquisition. Fraction of tRNA-bound form of  $\alpha$ Syn K/E<sub>6-60</sub> is calculated using densitometric analysis. **(lower)** Diffusion coefficient as a function of time measured for the  $\alpha$ Syn K/E<sub>6-60</sub> RNC during the cell extract titration. **(F)** <sup>1</sup>H,<sup>15</sup>N-SOFAST HMQC spectrum of  $\alpha$ Syn K/E<sub>6-60</sub> RNC in the presence (yellow) and absence (red) of 12.5 g/L *E. coli* cell extract. **(G)** Relative cross-peak intensities (RNC in cell extract vs. RNC in buffer) in varying concentrations of cell extract. **(H)** Anti- $\alpha$ Syn western blot in-cell NMR samples of  $\alpha$ Syn K/E<sub>6-60</sub> isolated protein and RNC (with wildtype and with arrest-enhanced SecM) following NMR data acquisition, cell lysis and sucrose cushion centrifugation. **(I)** <sup>1</sup>H,<sup>15</sup>N-SOFAST HMQC spectrum of <sup>2</sup>H,<sup>15</sup>N-labelled in-cell  $\alpha$ Syn K/E<sub>6-60</sub> RNC stalled using the wildtype SecM motif. **(J)** Relative cross-peak intensities (RNC vs isolated protein) of in-cell NMR samples. Although the C-terminus shows greater line broadening indicative of tethering to the ribosome, the large population of ribosome-released NC results in an averaged signal intensity profile with less well-defined broadenings associated with F94 and Y39, as observed with the arrest-enhanced RNC (see Fig 5E). **(K)** Summed 1D spectra of all acquired <sup>15</sup>N-SORDID spectra of in-cell samples of  $\alpha$ Syn K/E<sub>6-60</sub> isolated protein (left), RNC (middle) and arrest-enhanced RNC (right), using a diffusion delay of 300 ms to measure the fraction of intracellular species as indicated above each spectrum. **(L)** Correlation plot between relative cross-peak intensities (RNC relative to protein) in buffer and 1 molar equivalent of TF; different concentrations of *E. coli* cell extracts; in-cell (with arrest-enhanced SecM). Data were analysed with a simple linear fit (fitted line shown in plots). Analysis of data fittings, using a linear model  $y = ax + b$ . The gradient  $a$  can be related to the additional line broadenings observed under the conditions tested (relative to in buffer), where  $0 < a < 1$  indicates additional line broadening and therefore additional interaction or reduced flexibility, whereas  $a > 1$  indicates reduced line broadening and therefore reduced interaction or greater flexibility. In the case of in-cell line broadenings,  $a = 0$  would be an indication of a completely released NC population. The  $R^2$  value can be related to the differences in the locations of line broadenings within the protein sequence.

## NMR protocols and pulse sequences

As RNCs are prone to breakdown, we have developed a strategy to record small blocks of experiments interleaved with diffusion experiments, the latter informing on the integrity of the complex(14). We typically record spectra according to the below protocol:

Order	Experiment	Short description	Notes
1	zgesgp	1H spectrum	
2	stebpgp1spr	1H diffusion	Record at the beginning to rapidly assess quality of RNC sample
3	sfhmqcf3gpqh	First increment of a 2D SOFAST HMQC	
4	sfhmqcf3gpqh	2D SOFAST HMQC	
5	stebpgp1s19xn	15N diffusion	
6	zgesgp	1H spectrum	Repeat 5-8 until diffusion experiments indicate RNC breakdown
7	stebpgp1spr	1H diffusion	
8	(*)	2D spectrum of choice	

(\*) sfhmqcf3gpqh, hsqcetf3gpsi2.2.jk, or trosytf3gpsi2\_bsd\_tc.2.2.jk

The non-standard pulse sequences, hsqcetf3gpsi2.2.jk, and trosytf3gpsi2\_bsd\_tc.2.2.jk have been deposited on [BMRB](https://bmr.org) under BMRbig ID : bmrbig24. The web-link to the entry is <https://bmr.org/released/bmrbig24>.

## References

1. Koppel DE (1974) Study of Escherichia coli ribosomes by intensity fluctuation spectroscopy of scattered laser light. *Biochemistry* 13(13):2712–2719.
2. Dedmon MM, Lindorff-Larsen K, Christodoulou J, Vendruscolo M, Dobson CM (2005) Mapping long-range interactions in alpha-synuclein using spin-label NMR and ensemble molecular dynamics simulations. *J Am Chem Soc* 127(2):476–477.